

AD-A048 372

AIR FORCE CAMBRIDGE RESEARCH LABS HANSCOM AFB MASS

F/G 16/3

FLIGHT TEST DATA COMPARING ELECTRON ATTACHMENT BY ABLATION PROD--ETC(U)

1975

D T HAYES, S B HERSKOVITZ, J F LENNON

AFCRL-TR-75-0117

UNCLASSIFIED

| OF |
AD
A048372



NL

END
DATE
FILMED
2-78
DDC

AFCL-TR-75-0117

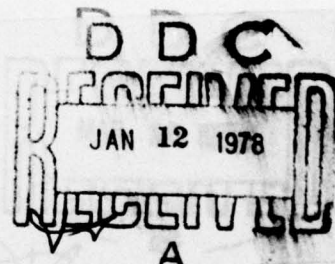


AD A 048372

AIAA PAPER
75-181

FLIGHT TEST DATA COMPARING ELECTRON ATTACHMENT BY
ABLATION PRODUCTS AND BY LIQUID INJECTION

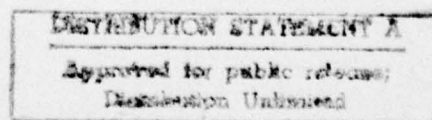
by
DALLAS T. HAYES, SHELDON B. HERSKOVITZ,
JOHN F. LENNON and J. LEON POIRIER
Air Force Cambridge Research Laboratories
Hanscom Airforce Base, Bedford, Massachusetts



AIAA 13th Aerospace Sciences Meeting

PASADENA, CALIF. / JANUARY 20-22, 1975

AD No. _____
DDC FILE COPY



For permission to copy or republish, contact the American Institute of Aeronautics and Astronautics,
1290 Avenue of the Americas, New York, N.Y. 10019.

(See 1473)

FLIGHT TEST DATA COMPARING ELECTRON
ATTACHMENT BY ABLATION PRODUCTS AND BY LIQUID INJECTION

Dallas T. Hayes
Sheldon B. Herskovitz
John F. Lennon*
J. Leon Poirier

Air Force Cambridge Research Laboratories
Hanscom AFB, Bedford, Massachusetts
01731

Abstract

Teflon ablation as a mechanism for altering the electron concentration in the flow surrounding a vehicle was examined under reentry conditions. This was a companion flight to a liquid injection test which used Freon 114B2. Data will be presented on the effect of the ablation products on the flow. These results will then be compared with those of the injection flight. Measurements were obtained by microwave techniques and paired electrostatic probe measurements of positive ion and electron densities. The results of both tests showed significant electron reduction with the dominant mechanism being negative ion formation.

Nomenclature

S/R_N	- Wetted length, normalized to nose radius
V	- Voltage
e	- electron charge
j	- current density
n	- particle number density
v	- thermal velocity
α	- angle of attack
ϵ_0	- permittivity of free space
λ	- sheath thickness
μ	- mobility

Introduction

Ablation is a widely accepted technique for providing thermal protection during reentry. Apart from this however, its use as a mechanism for altering the electron concentration in the surrounding flow was examined during the fifth in a series of rocket tests. Another alleviation technique, liquid injection, had already been tested under similar flight conditions.¹ The first

three^{2,3} flights established the nature of the unmodified reentry effects.

In this application, the initial thermal shielding resulting from the blowing off of the ablator into the boundary layer is not of major interest. It is the subsequent effect of the ablator products on the flow properties which must be considered. If sufficient mass has been added to the boundary layer, the resultant cooling can enhance recombination, thereby decreasing the electron concentrations which interfere with signal transmission during reentry. A more efficient technique than simple cooling is the use of chemicals with electrophilic properties. Less mass is required since the chemistry also includes the possibility of additional electrons being bound up as negative ions. These relatively massive ions interact only weakly with microwave radiation thus reducing the effect of the plasma. In the case of the liquid injection experiment, similar considerations applied. There the alleviant was locally introduced into the flow which would pass over the test antenna. Since the liquid injectant, Freon 114B2, undergoes rapid pyrolytic decomposition into a teflon-like monomer, the two flights represent conceptually different alleviation techniques which have similar flow chemistries.

The purpose of this paper is to report on the effect of the teflon (tetrafluoroethylene) ablation products on the flow and to compare these results with those of the injection flight. On both flights measurements were obtained by microwave techniques and paired electrostatic probes designed for separate measurement of positive ion and electron densities in the flow.

The reentry vehicles with the location of the electrostatic probes and microwave antennas are shown in Figure 1. The placement of the probes and antennas at various locations presents information on the time history of the effect of the ablated and injected materials as the flow progressed along the vehicle surface. The vehicles were blunt 90° cones with 6-inch nose radii. The hemispherical cap of the ablation flight was covered with teflon, selected for low alkali content. On the injection flight, as shown in the figure, the liquid was introduced from orifices located directly in front of the test antennas. The vehicles were spin stabilized

*Research Physicist, Member, AIAA

and reentered almost vertically. The ablation flight (angle of attack envelope, $|\alpha| = 12.8^\circ$) attained a peak velocity of 17,000 fps while the injection flight ($|\alpha| = 16.5^\circ$) reached 16,240 fps.

Injection and Ablation Mechanisms

Some description of the two techniques is essential to place the results in perspective. Details of the actual injection system have been given earlier.¹ The injection occurred in two phases. Between 280 kft and 180 kft, additive was injected in a series of seven 0.25 sec pulses at a 1 Hz rate. During these pulses the liquid was propelled by the expansion of a volume of air at one atmosphere pressure. It was expected that an approximately equal mass of additive would be injected during each pulse. In the second phase, a compressed nitrogen gas supply produced a controlled, time-varying increase in reservoir pressurization to compensate for the increasing external dynamic pressure. Activation of a high flow system resulted in a two-level injection mode with 0.25 sec high flow pulses immediately following the original low flow pulses. The increasing pressurization also tended to increase the injected mass flow of both modes. At high altitudes, low external pressures result in flash vaporization of most of the additive. At lower altitudes, however, this rapid evaporation becomes less important, and the liquid jet forms droplets with typical evaporation times of a few hundred microseconds.

In contrast to this complex internally controlled system, the teflon ablation represents a passive technique with the mass addition controlled by the heat of ablation of the selected heat shield material and the heat transfer associated with the vehicle geometry and flight dynamics. Estimates of the ablation at various altitudes were made using the laminar and turbulent heat transfer relations of Detra and Hidalgo.⁴ Since transition to turbulence on the nose would not occur until below 120 kft for the flight conditions, the ablation rates were generally low. Upon exposure to heat, the teflon decomposes directly into the gaseous state, yielding tetrafluoroethylene, C_2F_4 as the initial product.

After the alleviants are introduced into the surrounding air, the two approaches are compared with reference to their effects on the electron concentration profiles at the antenna and probe stations. The penetration of the liquid depends on the dynamic pressure ratios and was estimated by the formulation of Kolpin et al.⁵ which includes a vapor pressure correction term. The teflon, however, is ablated in a blowing off process from the surface and its mass addition is to the boundary layer of the vehicle.

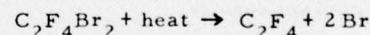
An initial estimate of the relative concentrations of alleviant to air was obtained. The penetration of the freon corresponded to the height of the entropy layer over the altitude range of inter-

est. The air mass flow for this layer was thus used as the reference condition at the vehicle shoulder. The teflon products were assumed to be uniformly mixed with this mass while the freon was compared to just the flow passing over the test antenna.

The combined results are shown in Figure 2. In the altitude range of interest for the microwave testing (below 250 kft), freon to air ratios from 100% to 1% were obtained. In addition, at the lower altitudes two different levels were injected. The corresponding teflon mole fractions were generally less than 10% and even less than 1% for a considerable range. It should be pointed out though, that the ablation results should be considered valid only at the higher altitudes. There an extensive part of the overall flow is taken up by the boundary layer. At the lower altitudes, however, the confinement of the boundary layer close to the wall would mean that the indicated ratios underestimate the actual additive levels. Similarly, the extent of the flow modified by the additive is also limited.

More complete specification of the two additive-ionized air interactions depends on a number of factors: solution of boundary layer equations including mass addition, characterization of the down-stream flow beyond the injection station, and better identification of the high temperature kinetics for the alleviant-air mixtures. The complexity of the situation can be seen by considering some of the factors involved in the chemistry.

The vaporized liquid injectant, chemically $C_2F_4Br_2$, is stable to about 900°K, at which temperature it undergoes pyrolysis by the reaction⁶



The tetrafluoroethylene intermediate, C_2F_4 , is the same compound that results from teflon decomposition. The oxidation chemistry is dependent upon several factors including relative concentration of the additive to air, thermal history, and incubation time in the flow field. Whereas the thermal and time histories of the additives are essentially similar, there are differences in the relative concentrations in the two experiments (Figure 2). As a result, some cooling effects were noted in the higher flow freon experiment (indicated by variations in negative bias probes). In addition, the differing molar concentrations produce variations in the expected oxidation chemistries. These factors, coupled with differing degrees of chemical equilibrium, represent areas which require additional consideration.

Probes and Antennas

To allow the data from the several flights to be compared, the experimental payloads for all the flights were similar. The basic microwave test systems and the diagnostic probes were located at identical vehicular positions on the teflon ablation

and liquid injection flight tests. This allows a direct comparison of the effect of the two alleviation techniques. The probe and microwave antenna locations are shown in Figure 1. On the liquid injection flight a probe was positioned at the same body station ($S/R_N = 1.77$) but displaced to the side of the injection ports. The purpose of this probe was to measure the positive ion density before the flow was modified by the liquid additive. From this measurement the electron density could be determined on the basis of total charge neutrality.

The flow was modified by alleviation materials for the remaining probe positions on the liquid injection flight and for all probes on the ablation flight. This resulted in at least a three component flow of ionized gas containing negative ions in addition to positive ions and electrons. In this case it is necessary to measure the electron density directly, and this was done through the use of positive biased probes. In addition, a number of probes were located in pairs to measure both the positive ion and electron density simultaneously.

On both flights, a probe pair was located at $S/R_N = 2.40$ between the low power transmitting and receiving antennas. On the ablation flight, an additional probe pair was situated just in front of the high power test antenna at $S/R_N = 1.77$. A probe was mounted at the telemetry antenna station ($S/R_N = 4.44$) to measure electron density on the liquid injection flight. The ablation flight carried a probe pair at the same location. As these probes were directly in line with the probes located at $S/R_N = 2.40$ on both flights, it was possible to compare the effect of the alleviation materials on the charge particle densities after a flow time of approximately 100 μ sec.

Two additional probes, which will not be discussed further in this report, were carried on each vehicle. On the liquid injection flight their purpose was to measure the spreading of the injectant plume as it flowed back over the vehicle. The plume effects, which were seen, have been reported elsewhere.¹ The two probes on the ablation flight confirmed the expectation that the ablation process was uniform circumferentially around the nose cap.

All probes were biased at $\pm 15V$ with the exception of the probe pair located on both flights at $S/R_N = 2.40$. Each probe in this pair was sequentially step biased at 15V and 30V positive or negative. According to the theory used to analyze the data, varying the probe bias varies the distance from the probe surface at which the charged particle density is measured.

A detailed discussion of the electrostatic probe theory has been presented in earlier reports.¹⁻³ Therefore, only a brief description of the technique used to analyze the probe data will be given.

During most of the altitude region of interest the charged particles undergo an appreciable

number of collisions with neutral particles in their passage through the probe sheath region to the collecting surface. Therefore, the probes were biased at a level ($|V| > 15V$) which laboratory tests⁷ and experience have shown is high enough to cause the bulk of the collisions to result in scattering in the forward direction. Thus the loss in probe current due to scattering out of the sheath region, is minimized. This loss is neglected and it is assumed that the full random flux of ionized particles of one sign will be collected. A planar probe and a planar sheath are also assumed. Under these conditions, the expression for the probe current is given by

$$j = (1/4) nev.$$

The planar space limited mobility controlled diode equation

$$j = (9/8) \epsilon_0 \mu \frac{V^2}{\lambda}$$

is used to locate the sheath edge. The probe equations apply only under current saturation conditions in a two component plasma, i.e. in a plasma consisting only of one type of positive ion and electrons. An additional constraint is that the probe bias is large enough to repel completely one species of particle while attracting all the particles of the other species which enter the probe sheath region. However, as the plasmas produced during these flights consisted of at least two types of negatively charged particles, the equations do not hold when the probe is biased positive to measure the negative current.

In the analysis of the data from the electrophilic flights, the effect of the negatively charged ions on the current collected by positive biased probes has been neglected when calculating the electron density. To justify this, a simple ad hoc theory of current collection in the presence of negative ions was developed.⁸ This theory showed that for the conditions achieved during the additive flight tests, the negative ion portion of the negative current may be neglected when determining the electron density, but must be included in the probe sheath thickness calculation.

Probe Results

The analysis of the probe data from the liquid injection flight has been reported.¹ However, this is the first time that results from the ablation flight have been discussed. Therefore, this section will begin with a discussion of typical probe data from two probe pairs on that flight test. Following this, the data from the liquid injection flight and the ablation flight will be compared.

Ablation Flight Test Data

The high power antenna probes were biased at 15V (one positive, the other negative), and the data are shown in Figure 3. The -15V probe became sensitive to the positive ion density at about

270 kft (409.5 sec) and the 15V probe began sensing the electron density at 240 kft (411.5 sec). The data missing from the positive ion curve late in the flight (420.0-422.0 sec) is due to the probe saturating.

The first thing noticed in Figure 3 is that the electron density is always at least two orders of magnitude less than the positive ion density. The positive ion density rose to a peak value of 10^{11} part./cm³ at approximately 210 kft. At this same time, the electron density was at its peak value of 4×10^8 part./cm³.

Consider now the amplitude of the modulation of the charged particle densities due to the spin of the vehicle and its nonzero angle-of-attack. On the injection flight, the densities varied by about a factor of five from the windward to leeward side. The degree of oscillation remained relatively constant until late in the flight when the angle of attack decreased due to atmospheric effects. On the ablation flight the modulation of the electron density was similar, remaining fairly constant at a factor of three. However, this trend was not followed by the positive ion density. At the beginning (~410.0 sec), the probe response was modulated by a factor of three, but in the period from 410.5 to 411.2 sec there was no apparent variation. After modulation returned, it increased to as much as a factor of eight at 413.6 sec with a subsequent decrease to 3 at 415.0 sec. It then remained constant. The decrease in oscillation at low altitudes could not be seen for this probe due to the saturation of the probe current after 420 sec. The initial loss at high altitudes (260-240 kft) cannot be explained with certainty but the same effect was observed in the data from all probes sensitive to the plasma during this altitude regime. It may be that the initiation of teflon ablation introduced some random effects.

Both probes show an increase in charged particle density at slightly below 120 kft (419 sec). This same increase, seen on all probes on the vehicle, is believed to be due to the onset of turbulence in the boundary layer. At about 90 kft the modulation amplitude decreases with the angle of attack. At 80 kft the electron density begins to drop. Here the vehicle's velocity is dropping below 10 kft/sec and both theoretical calculations and experience confirm that plasma effects are negligible for velocities below this value.

The telemetry antenna probe pair ($S/R_N = 4.44$) was of fixed bias ($\pm 15V$ respectively). The data are shown in Figure 4. The data from ion density probe show a slower buildup time (410-413 sec) than was the case for the probes located forward on the vehicle. However, as was true for the other ion probes, the normal windward-leeward modulation is missing during this time. Eventually (417 sec) the positive ion density reaches a value comparable to the value measured at the forward probes. This effect is contrary to the expected

result in that the ion density should decrease due to a natural relaxation, which would be the case in the absence of additive.

The data from the electron density probe shows an even more interesting result. At 200 kft the modulation character of the probe response changes. This is about the same altitude at which the reflection coefficient, measured by the TM test antenna, began to show a higher value between the windward and leeward positions than at either of those positions. Above 200 kft (<414 sec), the electron densities as measured by this probe are lower than the densities measured by the probes at the forward positions. Above 200 kft, as expected, the electron density is lower by a factor of 4 on the windward side. However, below 200 kft the opposite is the case. The electron densities at the rear of the vehicle are greater than at the forward positions. At 160 kft for example, the electron density is greater by a factor of 4 at $S/R_N = 4.44$. A somewhat similar result was seen on the liquid injection flight. However, on that flight the electron density at $S/R_N = 4.44$ was greater throughout the flight than that measured by probes directly behind the shoulder injection ports.

The increase in electron density at 120 kft is greater for this probe than for all other probes located forward on the vehicle. This is consistent with the supposition that this increase is due to turbulence. A turbulent boundary layer should first be triggered at the rear of the vehicle and thus have more time to develop at this most rearward station than those more forward on the vehicle.

Comparison of the Flight Test Results

Figure 5 presents the windward and leeward positive ion density measured at $S/R_N = 1.77$ on the liquid injection flight test and the corresponding data from the ablation flight. With the exception of two altitude regimes, there is good agreement between the data from both flights. The discrepancies exist where the ion density is increasing rapidly on the leeward side (260-220 kft) and for all data below 120 kft.

As the probe located at $S/R_N = 1.77$ on the injection flight was unaffected by the additive, the good agreement shows that the teflon ablation had no measurable cooling effect on the positive ion density. In fact, just the opposite effect is seen on the leeward side where the data from both flights do not agree. The ion density measured on the ablation flight is greater than that measured on the injection flight. The altitude regime where the disagreement is the greatest corresponds to that portion where the windward-leeward modulation disappeared.

The ion density data from the ablation flight are seen to increase below 120 kft. Transition to a turbulent boundary layer was predicted to occur around this altitude for both flights. No similar

trend was seen in the injection flight data.

Figure 6 shows the windward ion density measured at -30V bias by the probe at $S/R_N = 2.40$ on both flights. The dips in ion density seen occurring once each second in the injection flight data result from the pulsed injection of the liquid additive. A larger decrease occurred at 160 kft. after the high flow pulses were initiated. The peaks of the ion density occurring during the interpulse period are roughly equivalent to the expected ion density in the absence of additive. It is seen that the ion density measured on the ablation flight follow the peaks of the injection flight data with the exception of altitudes below 120 kft. This is a further indication that the ablation process had no perceptible cooling affect upon the flow.

Like the injection flight data for $S/R_N = 1.77$, no increase in charged particle density below 120 kft was seen for the injection flight. For all probes affected by the liquid additive, the result was similar to that shown in Figure 6 with no increase in either the electron density or the ion density in this altitude regime. Thus it appears that the mass addition from the ablation surface in the nose region does not represent a significant perturbation of the normally developed flow. However, the liquid additive is injected with a strong dynamic pressure component and may strongly alter the existing flow pattern and in addition, introduce considerable cooling. This could suppress the changes in electron density associated with an unperturbed transition to turbulent flow.

Figure 7 shows the leeward data from the same probes. Here the picture is quite different. Whereas the ablation flight data show ion densities roughly as would be expected if no ablation were present, the data from the liquid injection flight show that even in the interpulse periods, the ion density does not return to its unperturbed value. Excepted from this are the interpulse periods following the last high altitude low flow pulses (180-160 kft). The most pronounced effect of cooling is seen below 160 kft following the initiation of the high flow pulses. This effect slowly diminishes in intensity until around 100 kft where it disappears.

Figure 8 presents the electron density measured on both flights at $S/R_N = 2.40$. The disparity between the windward and leeward results is again apparent. Down to 160 kft, the windward electron density for the ablation flight falls midway between the successive maximum and minimum electron density values measured during the injection flight while it is greater or equal below this altitude. However, on the leeward side the electron density measured during the injection flight is always less than the ablation flight data.

Antenna Measurements

Measurements of the performance of microwave radiating systems during these flights are of

fundamental importance in obtaining information on the degree of improvement possible from the two flow modification techniques. The specific microwave measurements were antenna impedance mismatch, interantenna coupling, signal attenuation, and antenna pattern distortion. Whereas the probes measure the charged particle density at one position in the boundary layer, the microwave antenna response is sensitive to the integrated electron density across the shock layer. The analysis of these varied results gives considerable information on the changing flow structure.

The basic antenna test system for each flight consisted of a closely spaced pair of S-band slot antennas (2290.5 MHz) located near the shoulder of the nose cone. The transmitted signal was received both by the adjacent receiving antenna and by a number of ground receiving stations. The telemetry system also operated at S-band (2220.5 MHz) and allowed supplementary measurements to be made at the rear of the cone.

The incident and reflected power of the transmitting antennas were continuously monitored. Their ratio is the power reflection coefficient which gives an indication of the magnitude of the antenna impedance mismatch. The fraction of the power incident on the shoulder transmitting antenna which is ultimately received by the adjacent receiving antenna is the interantenna coupling. The coupling is generally decreased by the presence of ionization. The decrease is due to two factors. First, the transmitted signal is diminished by the mismatch. Second, the transmitted signal is attenuated by the ionization as it propagates to the receiving antenna. The ratio of the signal received on the ground to the incident signal, normalized to its value just before plasma effects set in, is the total signal attenuation. This gives the reduction in the strength of a signal as a result of its interaction with the electrons along the transmission path.

A number of comparisons can be made among the results of antenna performance for the alleviation flights and a reference flight on which the flow was unmodified. A few will be considered here.

The power reflection coefficients on the windward axis are compared in Figure 9. In the absence of additives, the reflection coefficient increased sharply to a value of about 0.9 at plasma onset and remained there down to about 100 kft. In contrast, the reflection coefficient observed on the freon flight did not exceed a value of about 0.3 on the windward side. The local minima in this curve correspond to the injection pulses of the freon. The response of the antenna for the teflon flight was intermediate to that of the freon and the reference flights. In the teflon case the maximum value was about 0.6. Thus both the chemical additives tended to suppress the antenna mismatch and improve antenna performance.

The corresponding curves for the leeward side were different in overall structure but showed a similar reduction in reflection coefficient. However, the variation in mismatch with spin was considerably more complex for the additive flights and indicates that the penetration and mixing of the additive is a sensitive function of angle of attack and body axis position.

The maximum change in interantenna coupling observed for the teflon ablation flight was not greatly different from that seen on the freon additive flight. However, the responses differed in two respects. First, there was no consistently large variation with spin in antenna coupling on the teflon flight as was observed on the freon flight. Though there was a brief initial maximum of 15 dB, the variation was less than a few dB for most of the flight. In contrast, the difference in values for the freon flight was from 6 to 8 dB for nearly all of the reentry trajectory. These results again demonstrate that the additive penetration, mixing, and subsequent quenching were strongly dependent on the three-dimensional flow structure.

The final test antenna system parameter to be discussed is the total signal attenuation which is shown in Figure 10. For the reference flight, the attenuation increased sharply at plasma onset and remained greater than 37 dB down to about 100 kft where data was lost as a result of effects from the aerodynamic heating. The corresponding curves for the teflon and freon flights differ in two respects. The first is that the growth in attenuation is more gradual when chemical additives are present, and second, the maximum attenuation is less. In Figure 10 the freon additive curve corresponds to the values of attenuation observed at the time of maximum freon effect. Decreases of up to 30 dB in the signal attenuation were observed as a result of the chemical additives.

The greater overall improvement for the freon additive displayed in Figures 9 and 10 was probably due, as discussed in a previous section, to the greater penetration depth of the freon. Microwave signals are sensitive to differences in additive mixing and penetration because they respond to integrated ionization levels across the entire shock layer. Even so, the data demonstrates that both freon injection and teflon ablation are effective methods of improving the performance of a microwave antenna system during reentry.

The reflection coefficient of the telemetry antennas was also suppressed by the chemical additives. There is one further alleviant aspect pertaining to the telemetry antennas which should be mentioned. The locally injected freon remained in a stream of small lateral extent. As the vehicle rotated, the cross flow caused the additive stream to alternately cover and partially uncover the telemetry antenna thus producing a large variation in reflection coefficient with spin. For the teflon flight, the additive is more uniformly distrib-

uted around the entire body and the variation in response with spin is considerably less.

Conclusions

Important plasma modification results were obtained from the successful AFCRL chemical alleviation flights. The paired probes provided information on the electron and ion concentrations both at the shoulder, the actual site of the microwave experiment, and at the rear of the vehicle, after an extended chemical reaction time. The conclusive result of these measurements is that the injection of freon and the ablation of teflon behaved principally as electrophilics. Although some cooling was observed in the case of freon injection, there was no indication of cooling in the teflon flight results.

Onboard diagnostic instrumentation demonstrated that the aerodynamic flow conditions were essentially identical in both flights.

On the teflon flight, probe data indicates that the electron density was at least two orders of magnitude lower than the positive ion density at all probe locations. In the freon flight, the electron density was lowered by as much as three orders of magnitude in certain cases. This, however, was partially due to cooling effects produced by the greater mass addition of liquid additive.

During the high altitude build-up phase of the positive charged particle density, the normal windward-leeward probe modulation was missing on the teflon flight. Other than this unexpected result, the electrostatic probes behaved normally and produced meaningful measurements down to 60 kft. The slowing of the vehicle and disappearance of plasma effects were noted. At 120 kft., all probes on the teflon flight showed an increase in charged particle density. Although transition to turbulence was predicted for both flights at this altitude, no such corresponding increase was noted on the freon flight.

Except for the cooling effects produced during actual liquid injection in the freon flight, windward positive ion and electron density measurements agreed very well on both flights. This was not the case, however, with the leeward data.

Both the teflon ablation and the freon injection reduced the mismatch of each of the onboard transmitting antennas. There was a marked decrease in signal attenuation for both the test and the telemetry antennas as a result of the additives. The change in interantenna coupling during reentry was similarly reduced.

The data comparisons for the two additive flights indicate that injection resulted in greater alleviation than ablation. However, it is apparent that either method represents a viable choice to improve the reentry performance of onboard antennas

References

1. Hayes, D.T., Herskovitz, S.B., Lennon, J.F. and Poirier, J.L. (1974) Electrostatic Probe Measurements of Chemical Injection Effects During a Reentry Flight Test, *Journal of Spacecraft and Rockets*, **11**: 388-394.
2. Poirier, J.L., Rotman, W., Hayes, D.T. and Lennon, J.F. (1969) Effects of the Reentry Plasma Sheath on Microwave Antenna Performance: Trailblazer II Rocket Results of 18 June 1967, AFCRL-69-0354.
3. Hayes, D.T. and Rotman, W., (1973), Microwave and Electrostatic Probe Measurements on a Blunt Reentry Vehicle, *AIAA Journal*, **11**: 675-682.
4. Detra, R.W. and Hidalgo, H. (1961) Generalized Heat Transfer Formulas and Graphs for Nose Cone Reentry into Atmosphere, *ARS Journal* **31**: 318-321.
5. Kolpin, M.A., Horn, K.P., and Reichenbach, R.E. (1968) Study of Penetration of a Liquid Injectant into a Supersonic Flow, *AIAA Journal* **6**: 853-858.
6. Skinner, G.B. and Ringrose, G.H., (1965) Shock-Tube Experiments on Inhibition of the Hydrogen-Oxygen Reaction, *J. of Chem. Physics*, **43**: 4129-4133.
7. Scharfman, W.E. and Bredfeldt, H.R. (1967) Experimental Studies of Electrostatic Probes for the Reentry Measurements Program-Phase B, Subcontract 611603 under Prime Contract 30-0690 AMC-333 (Y), SRI Project 6138, Stanford Research Institute, Menlo Park, California.
8. Hayes, D.T., Herskovitz, S.B., Lennon, J.F. and Poirier, J.L. (1974) Ablation Techniques for Enhancing Reentry Antenna Performance: Flight Test Results, AFCRL-TR-74-0572.

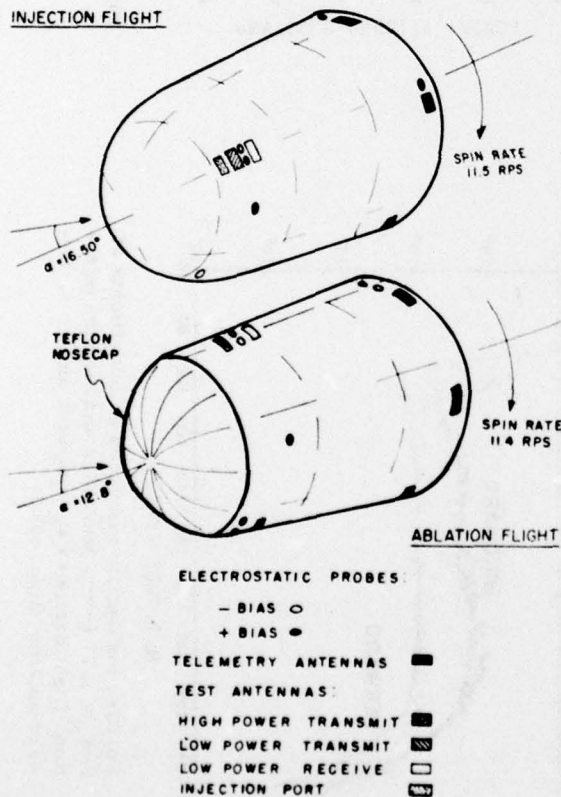


Figure 1. Sketch of nose cones showing location of probes and antennas.

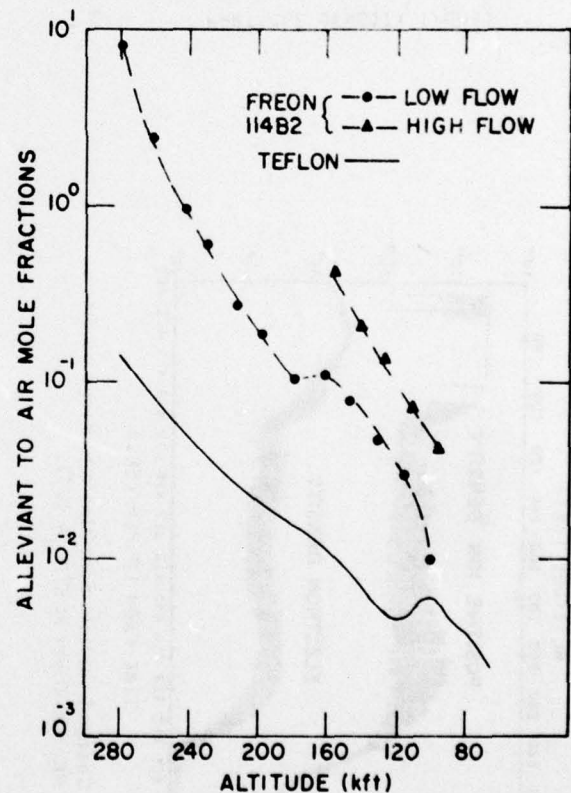


Figure 2. Ratio of alleviant to air for the two flights (mole fractions).

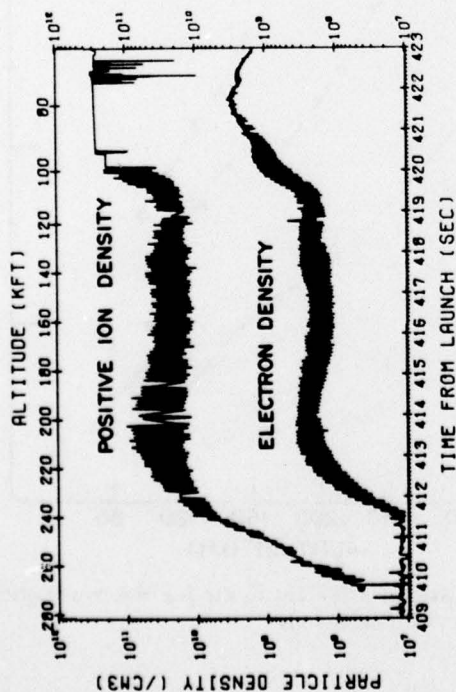


Figure 3. Charged particle densities measured on the ablation flight at $S/R_N = 1.77$.

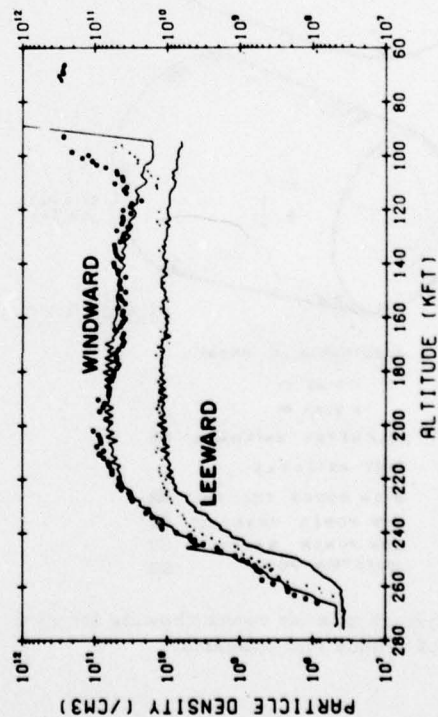


Figure 5. Positive ion density measured on both flights at $S/R_N = 1.77$ (—, windward and leeward injection flight data; ••••, windward and leeward ablation flight data).

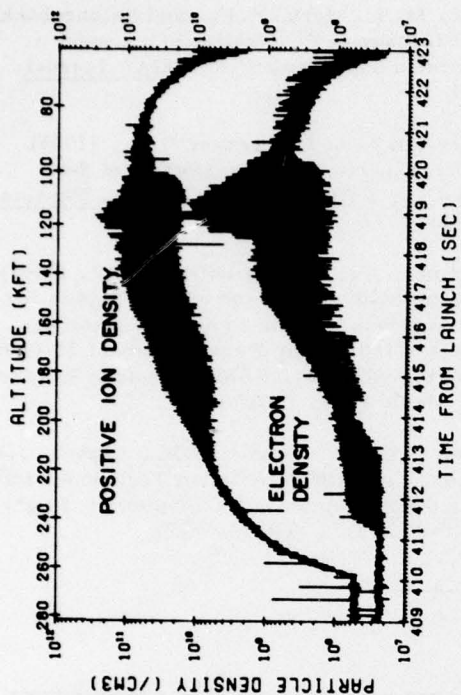


Figure 4. Charged particle densities measured on the ablation flight at $S/R_N = 4.44$.

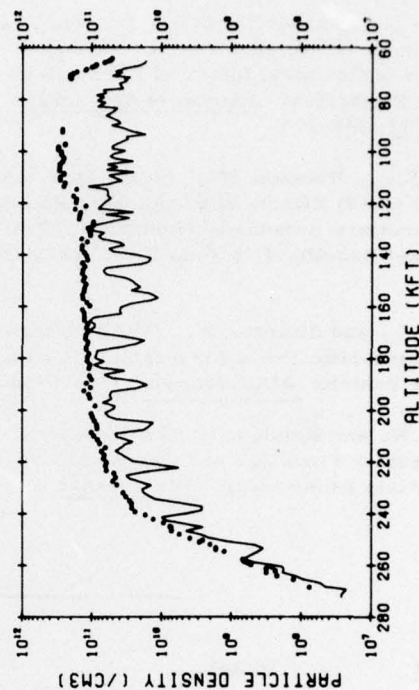


Figure 6. Windward positive ion density measured on both flights at $S/R_N = 2.4$ (—, injection flight data; ••••, ablation flight data).

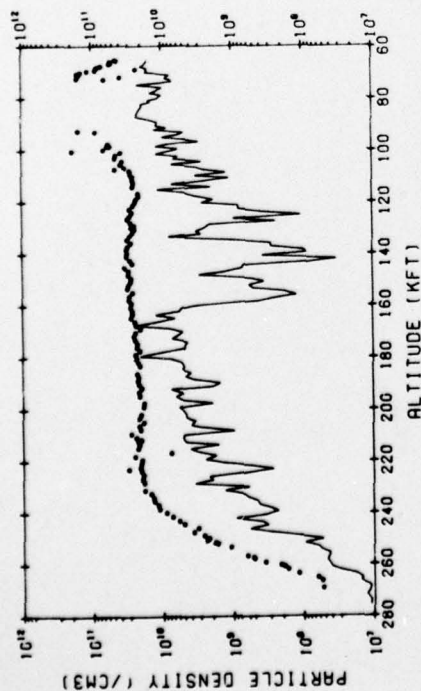


Figure 7. Leeward positive ion density measured on both flights at $S/R_N = 2.4$ (—, injection flight data; ····, ablation flight data).

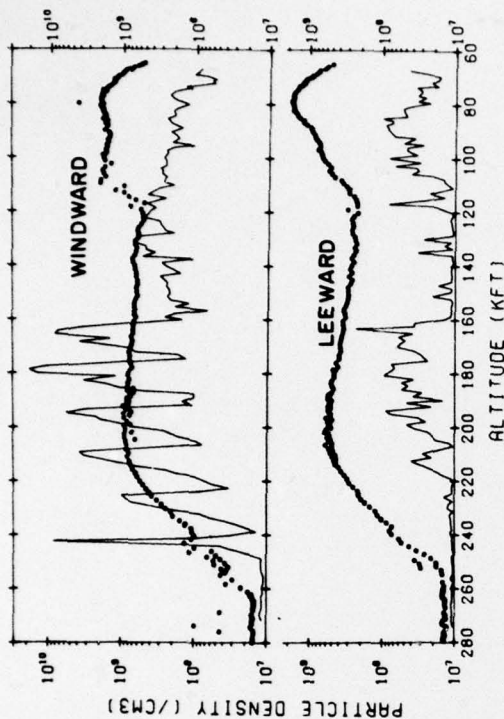


Figure 8. Windward and leeward electron density measured on both flights at $S/R_N = 2.4$ (—, injection flight data; ····, ablation flight data).

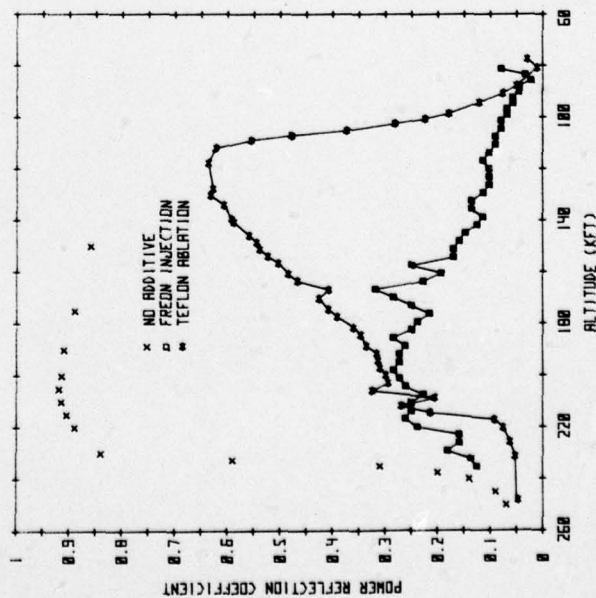


Figure 9.
Effect of alleviants
on power reflection
coefficient (wind-
ward data).

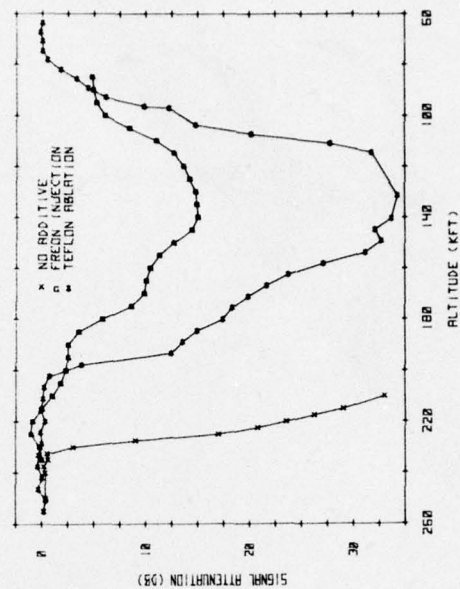


Figure 10. Effect of alleviants on total signal attenuation.